

A Three-State Model for the Polymorphism in Linear Tricobalt Compounds

Dimitrios A. Pantazis[‡] and John E. McGrady^{*†}

Contribution from WestCHEM, Department of Chemistry, University of Glasgow, Glasgow G12 8QQ, United Kingdom, and Department of Chemistry, University of York, Heslington, York YO10 5DD, United Kingdom

Received November 30, 2005; E-mail: j.mcgrady@chem.gla.ac.uk

Abstract: The remarkable polymorphism exhibited by the linear tricobalt compounds, $\text{Co}_3(\mu_3\text{-dpa})_4\text{Cl}_2$ and $\text{Co}_3(\mu_3\text{-dpa})_4\text{Br}_2$, can be explained using a model involving three distinct electronic states. At high temperatures, symmetric and unsymmetric forms arise from the population of doublet (^2A) and quartet (^4B) states, respectively, the latter containing a localized high-spin Co^{II} center. In the unsymmetric form, a reduction in temperature leads to a spin-crossover to a second quite distinct doublet state, ^2B , where, uniquely, the $d_{x^2-y^2}$ character on the localized Co^{II} center is distributed between the occupied and vacant manifolds. The variable population of the $\text{Co } d_{x^2-y^2}$ orbital gives rise to the continuous change in Co–Co and Co–N bond lengths as the temperature is decreased.

Introduction

Over the past decade, the properties of compounds containing chains of metal atoms have attracted a great deal of attention,¹ largely because of the potential applications of such systems as molecular-scale wires. Much of the work in this area has focused on polypyridylamine ligands, which have now been used to extend chains up to nine metal atoms.^{2–7} Within this series, trimetallic chains $\text{M}_3(\mu_3\text{-dpa})_4\text{X}_2$ (dpa = dipyridylamido, X = Cl, Br, M = Ni, Cu, Cr, Ru, Rh, and Co^{3-7}) are a particularly common motif, and their characterization naturally raises questions regarding the nature of the interaction between the metal atoms. The tricobalt compound, $\text{Co}_3(\text{dpa})_4\text{Cl}_2$,⁷ is a particularly challenging case due to the polymorphism of the Co_3 core, which can adopt either a symmetric structure with identical Co–Co separations ($s\text{-Co}_3(\text{dpa})_4\text{Cl}_2$) or a highly unsymmetric form ($u\text{-Co}_3(\text{dpa})_4\text{Cl}_2$) with one Co–Co bond up to 0.17 Å shorter than the other (Chart 1, Table 1), depending

on the number of molecules of dichloromethane in the unit cell (one and two for s - and $u\text{-Co}_3(\text{dpa})_4\text{X}_2$, respectively). The asymmetry in the Co–Co separations is also accompanied by significant changes in other parts of the molecule, most notably in the Co–N_{pyridine} bond lengths which are considerably longer at one end of the molecule (Co(3)–N = 2.119 Å) than the other (Co(1)–N = 1.978 Å).

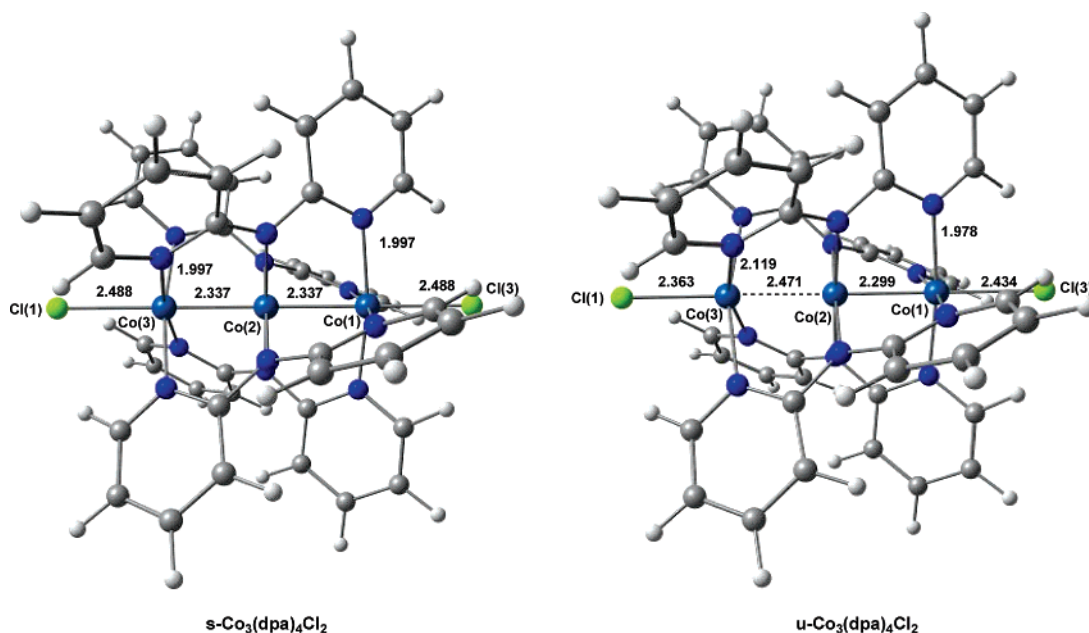
The magnetic properties of s - and $u\text{-Co}_3(\text{dpa})_4\text{Cl}_2$ offer some insight into the origins of the structural trends described above. At low temperatures, both symmetric and unsymmetric forms adopt doublet ground states, and both undergo spin-crossover as the temperature is increased, to $S = 5/2$ and $S = 3/2$ states, respectively. The long Co(3)–N bond lengths in $u\text{-Co}_3(\text{dpa})_4\text{Cl}_2$ (Chart 1) are highly characteristic of a localized high-spin ($S = 3/2$) Co^{II} center, suggesting that a monomer–dimer model, where the high-spin Co(3) center is linked to a diamagnetic Co(2)–Co(1) dimer,^{7a} is a reasonable first-order description of $u\text{-Co}_3(\text{dpa})_4\text{Cl}_2$. The temperature dependence of the structure of $u\text{-Co}_3(\text{dpa})_4\text{Cl}_2$,^{7f,i} however, hints at greater complexity; as the temperature is lowered, the spin-crossover to the doublet ground state is accompanied by a distinct reduction in the

[†] University of Glasgow.

[‡] University of York.

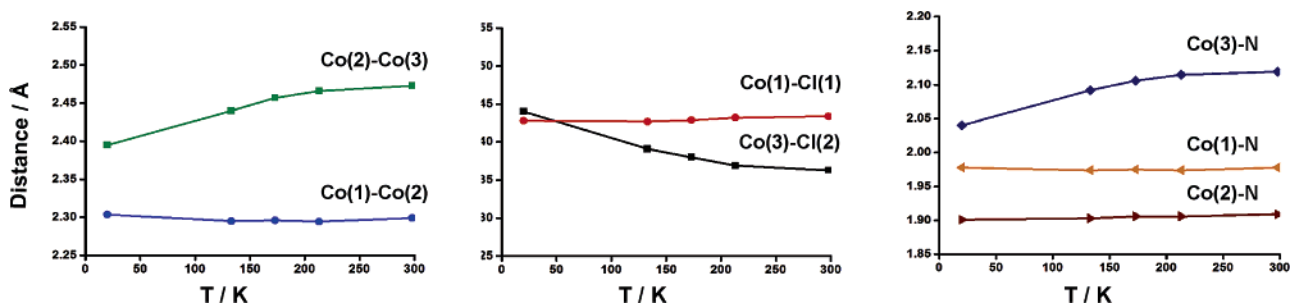
- (1) (a) Bera, J. K.; Dunbar, K. R. *Angew. Chem., Int. Ed.* **2002**, *41*, 4453. (b) Cotton, F. A. *Inorg. Chem.* **1998**, *37*, 5710. (c) Berry, J. F.; Cotton, F. A.; Murillo, C. A. *Organometallics* **2004**, *23*, 2503. (d) Lin, S.-Y.; Chen, L.-W. P.; Chen, C.-H.; Hsieh, M.-H.; Yeh, C.-Y.; Lin, T.-W.; Chen, Y.-H.; Peng, S.-M. *J. Phys. Chem. B* **2004**, *108*, 959.
- (2) (a) Peng, S.-M.; Wang, C.-C.; Jang, Y.-L.; Chen, Y.-H.; Li, F.-Y.; Mou, C.-Y.; Leung, M.-K. *J. Magn. Magn. Mater.* **2000**, *209*, 80. (b) Yeh, C. Y.; Chiang, Y.-L.; Lee, G.-H.; Peng, S.-M. *Inorg. Chem.* **2002**, *41*, 4096. (c) Shieh, S.-J.; Chou, C.-C.; Lee, G.-H.; Wang, C.-C.; Peng, S.-M. *Angew. Chem., Int. Ed. Engl.* **1997**, *26*, 56. (d) Cotton, F. A.; Daniels, L. M.; Lu, T.; Murillo, C. A.; Wang, X. *J. Chem. Soc., Dalton Trans.* **1999**, 517. (e) Berry, J. F.; Cotton, F. A.; Lei, P.; Lu, T.; Murillo, C. A. *Inorg. Chem.* **2003**, *42*, 3534.
- (3) Aduldecha, S.; Hathaway, B. J. *J. Chem. Soc., Dalton Trans.* **1991**, 993.
- (4) (a) Pyrka, G. J.; El-Mekki, M.; Pinkerton, A. A. *J. Chem. Soc., Chem. Commun.* **1991**, 84. (b) Wu, L.-P.; Field, P.; Morrissey, T.; Murphy, C.; Nagle, P.; Hathaway, B. J.; Simmons, C.; Thornton, P. *J. Chem. Soc., Dalton Trans.* **1991**, 993.
- (5) Clérac, R.; Cotton, F. A.; Daniels, L. M.; Dunbar, K. R.; Murillo, C. A.; Pascual, I. *Inorg. Chem.* **2000**, *39*, 748.
- (6) Sheu, J.-T.; Lin, C.-C.; Chao, I.; Wang, C.-C.; Peng, S.-M. *J. Chem. Soc., Chem. Commun.* **1996**, 315.

- (7) (a) Yang, E.-C.; Cheng, M.-C.; Tsai, M.-S.; Peng, S.-M. *J. Chem. Soc., Chem. Commun.* **1994**, 2377. (b) Cotton, F. A.; Daniels, L. M.; Jordan, G. T., IV. *J. Chem. Soc., Chem. Commun.* **1997**, 421. (c) Cotton, F. A.; Daniels, L. M.; Jordan, G. T., IV; Murillo, C. A. *J. Am. Chem. Soc.* **1997**, *119*, 10377. (d) Cotton, F. A.; Murillo, C. A.; Wang, X. *J. Chem. Soc., Dalton Trans.* **1999**, 3327. (e) Cotton, F. A.; Murillo, C. A.; Wang, X. *Inorg. Chem.* **1999**, *38*, 6294. (f) Clérac, R.; Cotton, F. A.; Daniels, L. M.; Dunbar, K. R.; Kirschbaum, K.; Murillo, C. A.; Pinkerton, A. A.; Schultz, A. J.; Wang, X. *J. Am. Chem. Soc.* **2000**, *122*, 6226. (g) Clérac, R.; Cotton, F. A.; Daniels, L. M.; Dunbar, K. R.; Murillo, C. A.; Wang, X. *J. Chem. Soc., Dalton Trans.* **2001**, 386. (h) Clérac, R.; Cotton, F. A.; Jeffery, S. P.; Murillo, C. A.; Wang, X. *Inorg. Chem.* **2001**, *40*, 1265. (i) Clérac, R.; Cotton, F. A.; Daniels, L. M.; Dunbar, K. R.; Murillo, C. A.; Wang, X. *Inorg. Chem.* **2001**, *40*, 1256. (j) Clérac, R.; Cotton, F. A.; Dunbar, K. R.; Lu, T.; Murillo, C. A.; Wang, X. *J. Am. Chem. Soc.* **2000**, *122*, 6226. (k) Clérac, R.; Cotton, F. A.; Dunbar, K. R.; Lu, T.; Murillo, C. A.; Wang, X. *Inorg. Chem.* **2000**, *39*, 3065. (l) Berry, J. F.; Cotton, F. A.; Murillo, C. A.; Roberts, B. K. *Inorg. Chem.* **2004**, *43*, 2277.

Chart 1. Structure of the $\text{Co}_3(\text{dpa})_4\text{Cl}_2$ Framework in s- and u- $\text{Co}_3(\text{dpa})_4\text{Cl}_2$ (298 K)**Table 1.** Optimized Structural Parameters for s- and u- $\text{Co}_3(\text{dpa})_4\text{Cl}_2$. States are Labeled According to the Common C_2 Point Group (labels for the D_4 point group are shown in parentheses where appropriate)

	Experiment			Theory				
	s- Co_3Cl_2		u- Co_3Cl_2	s- Co_3Cl_2		u- Co_3Cl_2		
	(298 K)	(298 K)	(20 K)	2A (2A_2)	2B (2E)	4A	4B	2A
configuration ^a				$a^{73/72}$ $b^{74/74}$	$a^{73/73}$ $b^{74/73}$	$a^{74/71}$ $b^{74/74}$	$a^{74/72}$ $b^{74/73}$	$a^{74/73}$ $b^{73/73}$
Cl(1)–Co(1)	2.488	2.434	2.428	2.449	2.514	2.418	2.415	2.502
Co(1)–Co(2)	2.337	2.299	2.304	2.337	2.298	2.318	2.319	2.318
Co(2)–Co(3)	2.337	2.471	2.385	2.337	2.298	2.432	2.449	2.424
Co(3)–Cl(2)	2.488	2.363	2.440	2.449	2.514	2.364	2.333	2.352
Co(1)–N	1.997	1.978	1.979	2.002	2.012	1.995	1.999	2.020
					2.003		1.994	1.999
Co(2)–N	1.907	1.909	1.902	1.926	1.930	1.935	1.945	1.945
					1.924		1.934	1.944
Co(3)–N	1.997	2.119	2.040	2.002	2.012	2.142	2.170	2.168
					2.003		2.156	2.160
$E(\text{rel})/\text{eV}$	BP86			0	+0.27	+0.58	+0.42	+0.80
	B3LYP ^b			0	+1.24	+0.29	+0.17	+0.76
	VS98 ^b			0	+0.04	−0.10	−0.18	+0.26

^a The nomenclature $a^{73/72}$ implies the presence of 73 spin- α electrons and 72 spin- β electrons in orbitals of a symmetry. ^b Energy evaluated using the BP86 optimized geometry and density.

**Figure 1.** Temperature dependence of the structural parameters of u- $\text{Co}_3(\text{dpa})_4\text{Cl}_2$.^{7f}

asymmetry of both Co–Co and Co–N bond lengths (Figure 1). Critically, the Co–Co, Co–Cl, and Co–N distances appear to vary *continuously* with temperature, a feature that is characteristic of a very flat potential energy surface, where lattice strain can induce significant distortions.⁸ Even at 20 K, however, the structure remains distinctly unsymmetric, despite the fact

that the ground state is clearly a doublet. Thus, it appears that there is a second, unsymmetric, doublet state that is quite distinct from the doublet ground state of s- $\text{Co}_3(\text{dpa})_4\text{Cl}_2$.

The structural evidence summarized in the previous paragraphs, along with clear magnetic evidence that both symmetric and unsymmetric forms have doublet ground states, has led to

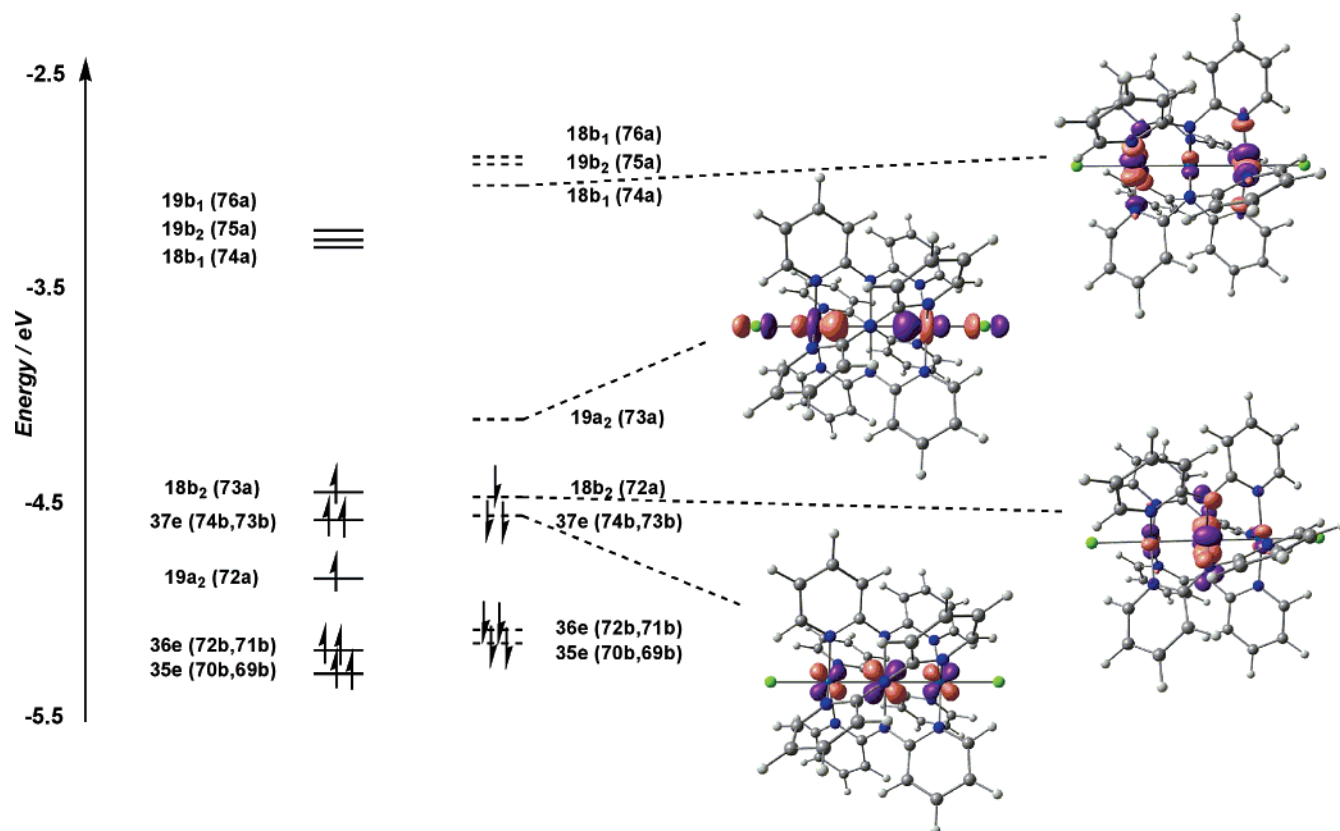


Figure 2. Molecular orbital array for the 2A_2 ground state of $s\text{-Co}_3(\text{dpa})_4\text{Cl}_2$. Orbitals are labeled according to the D_4 point group (labels appropriate to the C_2 point group are shown in parentheses).

speculation that these complexes represent a rare example of “bond-stretch isomerism”,⁹ the phenomenon where a molecule can exist in two distinct structural forms. This issue cannot, however, be resolved without a clear understanding of the electronic origins of the polymorphism. In a series of detailed studies of the electronic structure of these systems,¹⁰ Bénard and co-workers have shown conclusively that the global minimum is a symmetric doublet state containing a delocalized three-center–three-electron Co–Co–Co bond, and density functional theory reproduces the structure with encouraging accuracy. The structure of the unsymmetric form has been rather more difficult to rationalize, although a quartet state with structural parameters very similar to the 298 K structure of $u\text{-Co}_3(\text{dpa})_4\text{Cl}_2$ has been located, albeit at rather high energy relative to the symmetric global minimum.

The most pressing problem that remains to be resolved is the origin of the remarkable temperature dependence of the

structural and magnetic properties of $u\text{-Co}_3(\text{dpa})_4\text{Cl}_2$. In particular, how can we reconcile the unsymmetric structure, with the clear structural signature of a high-spin ($S = 3/2$) Co^{II} center, with the magnetic data that indicate a doublet ground state? Cotton has remarked that “our understanding of metal–metal bonding cannot be considered complete until it is able to deal with a case like this”.⁷¹ In this contribution, we present an electronic model based on *three* distinct electronic states, which can account for all the experimental observations detailed in the preceding paragraphs. Specifically, the model embraces (a) the presence of a low-lying unsymmetric quartet state, (b) the presence of distinct symmetric and unsymmetric doublet states, and (c) the remarkable temperature dependence of the structure of the unsymmetric form.

Results and Discussion

Electronic Structure of $s\text{-Co}_3(\text{dpa})_4\text{Cl}_2$ (2A_2 Ground State).

The electronic structure of the doublet ground state of $s\text{-Co}_3(\text{dpa})_4\text{Cl}_2$ has been extensively discussed by Bénard and co-workers,¹⁰ and we offer only a brief discussion here to highlight the key features that are relevant to the subsequent discussion. The global minimum is a D_4 -symmetric doublet (2A_2), and the optimized structural parameters (Table 1) are in good agreement with all the available X-ray data for $s\text{-Co}_3(\text{dpa})_4\text{Cl}_2$, with relatively short Co–Co (2.33 Å) and Co–N (2.00, 1.94 Å) bonds.¹¹ The molecular orbital array, summarized in Figure 2, confirms the presence of a three-center–three-electron bond, with one unpaired electron in a nonbonding orbital of a_2

- (8) (a) Burgi, H. B. *Inorg. Chem.* **1973**, *12*, 2321. (b) Stranger, R.; Smith, P. W.; Grey, I. E. *Inorg. Chem.* **1989**, *28*, 1271. (c) McGrady, J. E.; Lovell, T.; Stranger, R. *Inorg. Chem.* **1997**, *36*, 3242. (d) Wijnands, P. E. M.; Wood, J. S.; Reedijk, J.; Maaskant, W. J. A. *Inorg. Chem.* **1996**, *35*, 1214. (e) Simmons, C. J.; Stratemeier, H.; Hanson, G. R.; Hitchman, M. A. *Inorg. Chem.* **2005**, *44*, 2753.
- (9) (a) Stohrer, W.-D.; Hoffmann, R. *J. Am. Chem. Soc.* **1972**, *94*, 779. (b) Stohrer, W.-D.; Hoffmann, R. *J. Am. Chem. Soc.* **1972**, *94*, 1661. (c) Jean, Y.; Lledos, A.; Burdett, J. K.; Hoffmann, R. *J. Am. Chem. Soc.* **1988**, *110*, 4506. (d) Song, J.; Hall, M. B. *Inorg. Chem.* **1991**, *30*, 4433. (e) Parkin, G. *Chem. Rev.* **1993**, *93*, 887. (f) Parkin, G. *Acc. Chem. Res.* **1992**, *25*, 455. (g) McGrady, J. E. *Angew. Chem., Int. Ed.* **2001**, *39*, 3077. (h) Boatz, J. A.; Gordon, M. S. *Organometallics* **1996**, *15*, 2118. (i) Nguyen, K. A.; Gordon, M. S.; Boatz, J. A. *J. Am. Chem. Soc.* **1994**, *116*, 9241. (j) Pietsch, M. A.; Hall, M. B. *J. Phys. Chem.* **1994**, *98*, 11373. (k) Filatov, M.; Shaik, S. *J. Phys. Chem. A* **2000**, *104*, 6628.
- (10) (a) Rohmer, M.-M.; Bénard, M. *J. Am. Chem. Soc.* **1998**, *120*, 9372. (b) Rohmer, M.-M.; Strich, A.; Bénard, M.; Malrieu, J.-P. *J. Am. Chem. Soc.* **2001**, *123*, 9126. (c) Rohmer, M.-M.; Bénard, M. *Chem. Soc. Rev.* **2001**, *30*, 340.

- (11) The optimized bond lengths summarized for the 2A_2 state in Table 1 are almost identical to those reported by Rohmer and Bénard in ref 10a.

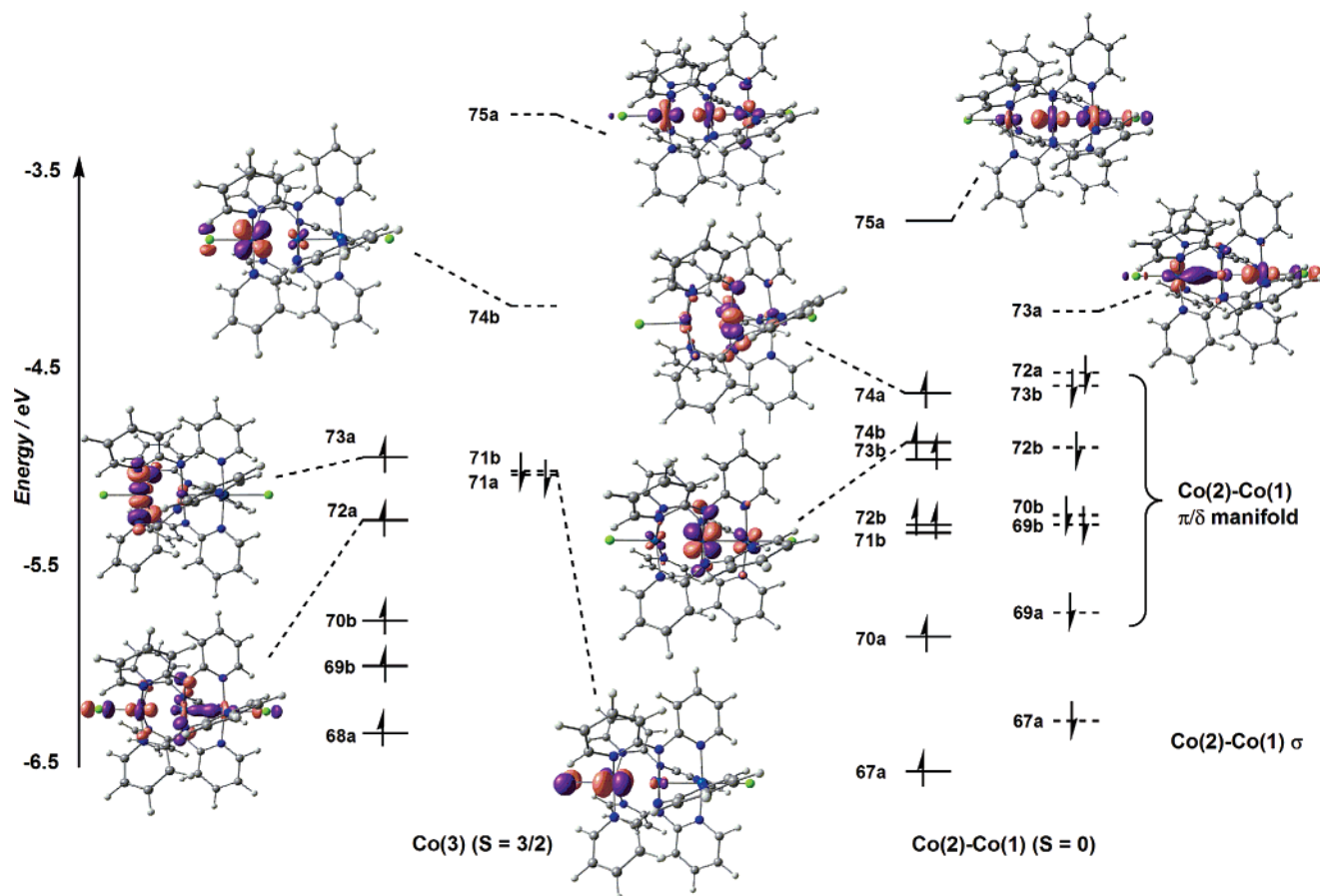


Figure 3. Molecular orbital array for the 4B state of $u\text{-Co}_3(\text{dpa})_4\text{Cl}_2$. Orbitals localized on the isolated Co(3) center are shown on the left, those localized on the Co(2)–Co(1) dimer on the right. The 4A state reported by Bénard and co-workers can be obtained by promoting an electron from 71a β to 74b β .

symmetry ($19a_2$), giving a 2A_2 ground state (2A in C_2 symmetry). Rohmer and Bénard have also previously discussed two distinct low-lying excited states, 2E and 2B_2 , arising from $37e\beta \rightarrow 19a_2\beta$ and $18b_2\beta \rightarrow 19a_2\beta$ transitions, respectively. The first of these plays an important role in the development of our model for the temperature-dependent behavior of $u\text{-Co}_3(\text{dpa})_4\text{Cl}_2$, and so merits further consideration. The orbitally degenerate 2E state is clearly unstable with respect to a first-order Jahn–Teller distortion, and indeed a small rhombic distortion ($\Delta\text{Co(3)}\text{–N} = 0.009 \text{ \AA}$) gives rise to a C_2 -symmetric 2B state, 0.03 eV lower in energy. As Jahn–Teller distortions will play an important role in the subsequent discussion, we use the lowest common sub-group, C_2 , to label the symmetries of all orbitals and states throughout this manuscript.

High-Temperature Form of $u\text{-Co}_3(\text{dpa})_4\text{Cl}_2$: Electronic Structure of the Quartet Potential Energy Surface. Within the constraints of C_4 point symmetry, we have located two distinct quartets, the 4A state reported by Bénard and Rohmer, and an orbitally degenerate 4E , both of which show the highly unsymmetric Co–Co separations and elongated Co(3)–N bonds characteristic of $u\text{-Co}_3(\text{dpa})_4\text{Cl}_2$. The net spin densities on Co(3) of 2.19 (4A) and 2.21 (4E) confirm the presence of a localized high-spin ($S = 3/2$) Co^{II} center in both cases. The two states are almost degenerate, lying 0.59 eV above the symmetric doublet ground state, but the 4E state is Jahn–Teller unstable, and a rhombic distortion leads to a C_2 -symmetric 4B state 0.17 eV lower in energy. In the molecular orbital array for the 4B state shown in Figure 3, the orbitals are separated based both

on their spins (α or β) and also on their localization. On the right-hand side, the orbital array is typical of a diamagnetic $\text{Co}^{\text{II}}\text{–Co}^{\text{II}}$ dimer (net spin densities 0.01 and 0.20 on Co(2) and Co(1), respectively), with a fully occupied π/δ manifold separating the Co–Co σ ($67a\alpha/\beta$) and σ^* ($75a\alpha$, $73a\beta$) set.¹² The left-hand side of the diagram, in contrast, is typical of a high-spin Co^{II} ion (net spin density 2.33), with five spin- α and two spin- β orbitals in the occupied manifold. From a structural perspective, the most significant feature of the diagram is the presence of a single electron in the Co(3) $d_{x^2-y^2}$ orbital ($73a\alpha$), which is responsible for the elongation of the Co(3)–N bonds. The influence of the Jahn–Teller distortion is most apparent in the orbitals localized on Co(3), where the previously degenerate $d_{xz/yz}$ pair, 71b β and 74b β , are split by almost 1 eV.

While the gross features of the 4B state suggest that it can be viewed, to a first approximation, as a high-spin $S = 3/2$ Co(3) center coupled to a diamagnetic Co(2)–Co(1) dimer, the orbitals on the two sides are significantly mixed, particularly within the σ framework. This mixing is most apparent between the vacant spin- β components of Co(3) d_{z^2} and Co(2)–Co(1) σ^* , which are destabilized by the effects of spin polarization on Co(3) and antibonding overlap on the Co(2)–Co(1) dimer, respectively. As a result of this mixing, the $73a\beta$ orbital is extensively delocalized over the trinuclear framework and becomes almost nonbonding. In contrast, the corresponding spin- α orbital, $75a$

(12) (a) Cotton, F. A.; Feng, X. *Inorg. Chem.* **1989**, *28*, 1180. (b) Cotton, F. A.; Daniels, L. M.; Feng, X.; Maloney, D. J.; Matonic, J. H.; Murillo, C. A. *Inorg. Chim. Acta* **1997**, *256*, 291.

α remains localized on the Co(1)–Co(2) unit and lies significantly higher in energy. As we show later, the stabilization of the 73a β orbital, which lies only 0.2 eV above the occupied manifold, plays a key role in the temperature-dependent behavior of the unsymmetric structure.

Our description of the quartet manifold of $u\text{-Co}_3(\text{dpa})_4\text{Cl}_2$ differs only subtly from that published previously, in that we have identified a second quartet state (^4B). In previous work, Bénard and Rohmer argued that the ^4A state was unlikely to play a role in any of the observed structural chemistry due to its relatively high energy (0.59 eV above the symmetric ^2A ground state).¹⁰ The strong Jahn–Teller stabilization of the ^4B state (0.17 eV) makes it a far more viable candidate in this regard. Moreover, it is not clear that the energies calculated using the BP86 functional¹³ (or indeed any other) provide a reliable estimate of the relative stabilities of states of different multiplicity, particularly where the electron density distributions differ significantly. There has been a lively debate in the recent literature regarding the ability of different functionals to model spin-state changes,¹⁴ and Baerends and co-workers have also noted the overstabilization of multicenter–three-electron bonds (such as that in the ^2A state) by gradient-corrected functionals.¹⁵ These uncertainties prompted us to recalculate the relative energies of the ^2A and ^4B states using a range of functionals (in each case, energies were calculated using the optimized geometries and converged densities from the BP86 functional). The data summarized in Table 1 clearly indicate that both the hybrid (B3LYP¹⁶) and meta-GGA (VS98¹⁷) functionals strongly stabilize the ^4B state relative to ^2A , and the VS98 functional even reverses their order. It is not our intention to debate the relative merits of different functionals, but simply to note that the possibility that the ^4B state plays a role in the structural chemistry cannot be dismissed solely on the grounds of its relatively high energy at the BP86 level.

Temperature Dependence of the Structure of $u\text{-Co}_3(\text{dpa})_4\text{Cl}_2$: Spin-Crossover to the Doublet Potential Energy Surface. While the computed properties of the ^4B state are fully consistent with both the structural and magnetic properties of $u\text{-Co}_3(\text{dpa})_4\text{Cl}_2$ at 298 K, the variations in structure as the temperature is lowered to 20 K remain a challenge. To reiterate the experimental evidence, the magnetic data indicate a spin-crossover to an $S = 1/2$ ground state below 200 K, which is accompanied by a reduction in the asymmetry of the Co–Co–Co core and a continuous contraction of the Co(3)–N bonds. Using the molecular orbital diagram of the ^4B state (Figure 3) as a reference point, there are a number of ways to generate a doublet. Promotion of an electron from the 73a α orbital to 74b β corresponds to an $S = 3/2 \rightarrow S = 1/2$ spin-crossover localized on the isolated Co(3) center. Such a transition would regenerate

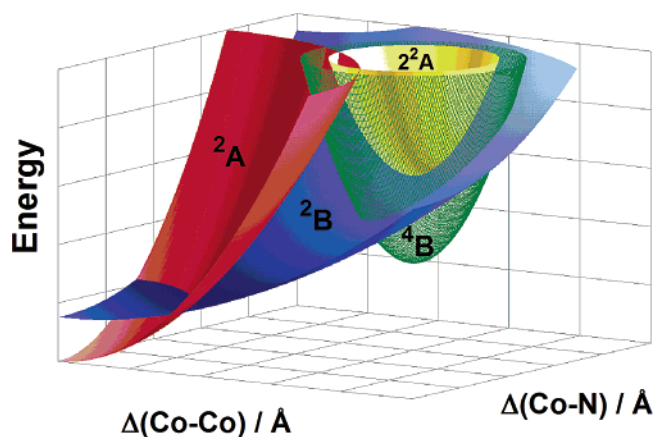


Figure 4. Schematic representations of the potential energy surfaces for ^2A , ^4B , ^2A , and ^2B states of $\text{Co}_3(\text{dpa})_4\text{Cl}_2$.

the configuration of the ^2A ground state ($a^{73/72}b^{74/74}$) and therefore naturally lead to an equalization of both Co–Co and Co–N bond lengths. However, the minima for the ^2A and ^4B states lie in very different regions of multidimensional space (shown schematically in Figure 4), suggesting that the conical intersection between the two potential energy surfaces will be at high energy. In such circumstances, it is difficult to rationalize the continuous variation in the Co(3)–N bond lengths between 170 and 20 K, which is indicative of a very flat potential energy surface.

In the previous section, we highlighted the strong mixing between the spin- β components of the Co(3) $d_{x^2-y^2}$ and Co(1)–Co(2) σ^* orbitals, which makes the 73a β orbital almost nonbonding (Figure 3). In fact, it is this orbital, rather than 74b β , that forms the LUMO of the ^4B state, and so promotion of an electron into 73a β from the spin- α manifold offers an alternative mechanism for the generation of low-lying doublet states. Critically, this mechanism does not necessarily depopulate the Co(3) $d_{x^2-y^2}$ orbital, thus allowing the doublet states to retain the long Co(3)–N bonds that are diagnostic of a high-spin Co^{II} center. In the following paragraphs, we analyze the structural and electronic properties of two distinct doublet states that can arise through this mechanism, one where the electron is transferred from the highest occupied orbital of b symmetry in the ^4B manifold (74b α in Figure 3), the other where the donor orbital has a symmetry (74a α).

Electronic Structure of the ^2A State. Starting from the ^4B state shown in Figure 3, the transfer of a single electron from the 74b α orbital into 73a β gives rise to a second state with ^2A symmetry, ^2A . It is important to emphasize that, although the ^2A and ^2A states share the same symmetry, their electronic configurations are quite distinct: $a^{73/72}b^{74/74}$ for ^2A and $a^{74/73}b^{73/73}$ for ^2A . In fact, ^2A and ^2A are formally related by a two-electron excitation, precisely the situation in the tricycloalkanes that constitute the “classic” example of bond-stretch isomerism^{9a} and also in the ruthenium dimer, $(\text{CpRu})_2(\mu\text{-Cl})_2$, that we discussed recently.^{9b} The optimized structure of the ^2A state (Table 1) retains the long Co(3)–N bonds characteristic of the high-spin Co^{II} center as well as the distinct asymmetry in the Co–Co bonds. In fact, the structures of the ^4B and ^2A states are remarkably similar, with the exception of the Co(1)–Cl(1) bond, which is elongated in ^2A as a result of the Co–Cl σ^* character in 73a β . The net spin densities of 2.26 [Co(3)], -0.60 [Co(2)], and -0.89 [Co(1)] confirm that ^2A is a broken-

- (13) (a) Becke, A. D. *Phys. Rev. A* **1988**, *38*, 3098. (b) Perdew, J. P. *Phys. Rev. B* **1986**, *33*, 8822.
- (14) (a) Swart, M.; Groenhof, A. R.; Ehlers, A. W.; Lammertsma, K. *J. Phys. Chem. A* **2004**, *108*, 5479. (b) Chang, C. H.; Boone, A. J.; Bartlett, R. J.; Richards, N. G. *J. Inorg. Chem.* **2004**, *43*, 458. (c) Reiher, M.; Salomon, O.; Hess, B. A. *Theor. Chem. Acc.* **2001**, *107*, 48. (d) Paulsen, H.; Duelund, L.; Winkler, H.; Toftlund, H.; Trautwein, A. X. *Inorg. Chem.* **2001**, *40*, 2201. (e) Chen, G.; Espinosa-Perez, G.; Zentella-Dehesa, A.; Silaghi-Dumitrescu, I.; Lara-Ochoa, F. *Inorg. Chem.* **2000**, *39*, 3440. (f) Harris, D.; Loew, G. H.; Kormornicki, A. *J. Phys. Chem. A* **1997**, *101*, 3959–3965.
- (15) Gruning, M.; Gritsenko, O. V.; van Gisbergen, S. J. A.; Baerends, E. J. *J. Phys. Chem. A* **2001**, *105*, 9211.
- (16) (a) Becke, A. D. *J. Chem. Phys.* **1993**, *98*, 5648. (b) Watson, M. A.; Handy, N. C.; Cohen, A. J. *J. Chem. Phys.* **2003**, *119*, 6475.
- (17) Van Voorhis, T.; Scuseria, G. E. *J. Chem. Phys.* **1998**, *109*, 400.

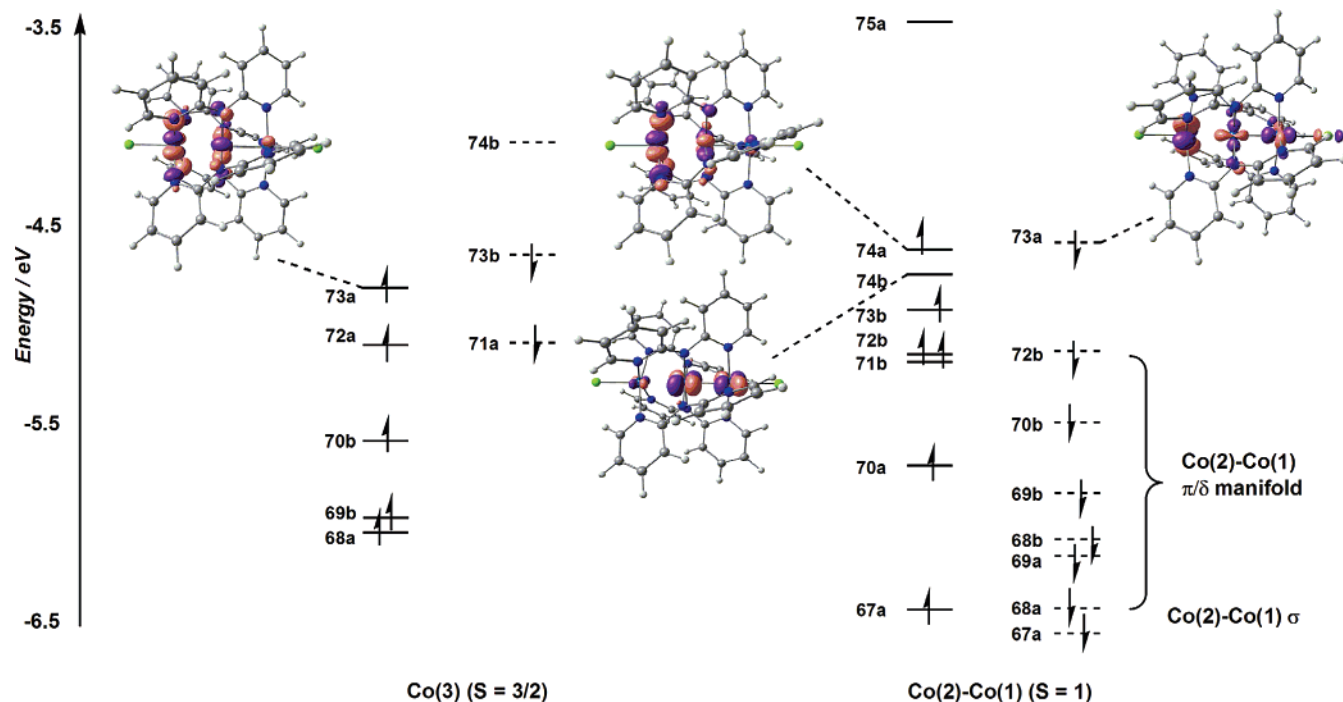


Figure 5. Molecular orbital array for the 2^2A state of $\text{Co}_3(\text{dpa})_4\text{Cl}_2$. Orbitals localized on the isolated $\text{Co}(3)$ center are shown on the left, those localized on the $\text{Co}(2)\text{--Co}(1)$ dimer on the right.

symmetry state containing an isolated $S = 3/2$ Co^{II} center, antiferromagnetically coupled to a $\text{Co}\text{--Co}$ dimer in an $S = 1$ state. The broken-symmetry nature of solution leads to significant spin contamination: $\langle S^2 \rangle = 2.37$, compared to a value of 0.75 for a pure doublet and 2.75 for an idealized antiferromagnetically coupled $S = 3/2 \times S = 1$ system.^{18,19}

Despite the fact that the 2^2A state exhibits the gross structural and electronic properties of the low-temperature form of $\text{u-Co}_3(\text{dpa})_4\text{Cl}_2$ (i.e., it is an unsymmetric doublet), a more detailed examination of its electronic structure does not support the proposal that it plays a role in the observed structural chemistry. Most obviously, it has a non-aufbau configuration, with the vacant 74b α orbital lying below occupied 74a α . Furthermore, while different functionals again influence the relative energies of the different states (Table 1), the 2^2A state remains significantly (0.39–0.59 eV) higher than 4^B in all cases. Finally, and most importantly, the $\text{Co}(3)$ $d_{x^2-y^2}$ orbital remains fully occupied, and so the 2^2A state offers no simple explanation for the remarkable temperature dependence of the $\text{Co}\text{--Co}$ and $\text{Co}\text{--N}$ bond lengths.

Electronic Structure of the 2^2B State. Starting from the non-aufbau configuration of the 2^2A state (Figure 5), a second doublet with 2^2B symmetry can be accessed by transfer of an electron from 74a α to 74b α , giving the configuration $a^{73/73}b^{74/73}$. A single point calculation at the 2^2A geometry indicates that the 2^2B surface lies 0.07 eV lower than 2^2A at this point, but all attempts to identify an unsymmetric local minimum for this state have proved unsuccessful. In all cases, the geometry reverts to a symmetric form with short $\text{Co}(3)\text{--N}$ and $\text{Co}(1)\text{--N}$ bonds, indicating that the potential energy surface connecting the symmetric and unsymmetric limits does not feature any

maxima in the case of the 2^2B state. The smooth convergence to a symmetric structure can be simply explained in symmetry terms by noting that the $a^{73/73}b^{74/73}$ configuration is identical to that for the Jahn–Teller-distorted 2^2B excited state of the symmetric system discussed earlier. This contrasts with the two states of 2^2A symmetry (2^2A and $2^2A'$), which differ in configuration, giving rise to two distinct minima separated by a substantial barrier. The 2^2B state is therefore unique in allowing a smooth correlation between the symmetric and unsymmetric limits (shown schematically in Figure 4).

We have thus far emphasized the asymmetry of the $\text{Co}\text{--Co}$ bonds, but the composition of the orbitals in the 2^2B state offers an important insight into the origin of the *continuous* variation in $\text{Co}\text{--N}$ bond lengths in $\text{u-Co}_3(\text{dpa})_4\text{Cl}_2$. In the 2^2A state (Figure 5), $\text{Co}(2)$ d_{xy} and $\text{Co}(3)$ $d_{x^2-y^2}$ ($\text{Co}\text{--N}$ σ^*) character is evenly distributed between the 73a α and 74a α orbitals, the two atomic orbitals being nonorthogonal as a result of the helical twist imposed by the dpa ligands. In the 4^B state, in contrast, $\text{Co}(3)$ $d_{x^2-y^2}$ character is largely localized in 73a α and $\text{Co}(2)$ d_{xy} in 74a α . The different distribution of $\text{Co}(3)$ $d_{x^2-y^2}$ and $\text{Co}(2)$ d_{xy} character between these two molecular orbitals does not, however, have any significant impact on the structure in either case because both 73a α and 74a α are occupied. In the 2^2B state, in contrast, only 73a α is occupied, and the $\text{Co}(3)\text{--N}$ bond length will therefore depend critically on the amount of $\text{Co}(3)$ $d_{x^2-y^2}$ character in this orbital. The 2^2B potential energy surface is therefore unique in providing an electronic mechanism that can account for a *continuous* variation in the population of the $\text{Co}(3)$ $d_{x^2-y^2}$ orbitals and, hence, in the $\text{Co}(3)\text{--N}$ bond lengths between the characteristic high-spin (ca. 2.15 Å) and low-spin (ca. 2.00 Å) limits.

The effect of varying the $\text{Co}(3)$ $d_{x^2-y^2}$ character in the occupied manifold can be modeled by adjusting the occupations of the 73a α and 74a α orbitals from 1.0:0.0 (the configuration

(18) (a) Dai, D.; Whangbo, M.-H. *J. Chem. Phys.* **2001**, *114*, 2887. (b) Dai, D.; Whangbo, M.-H. *J. Chem. Phys.* **2003**, *118*, 29.

(19) In contrast, the $\langle S^2 \rangle$ value of 3.79 for the 4^B state (exact value 3.75) confirms the absence of significant spin contamination in this case.

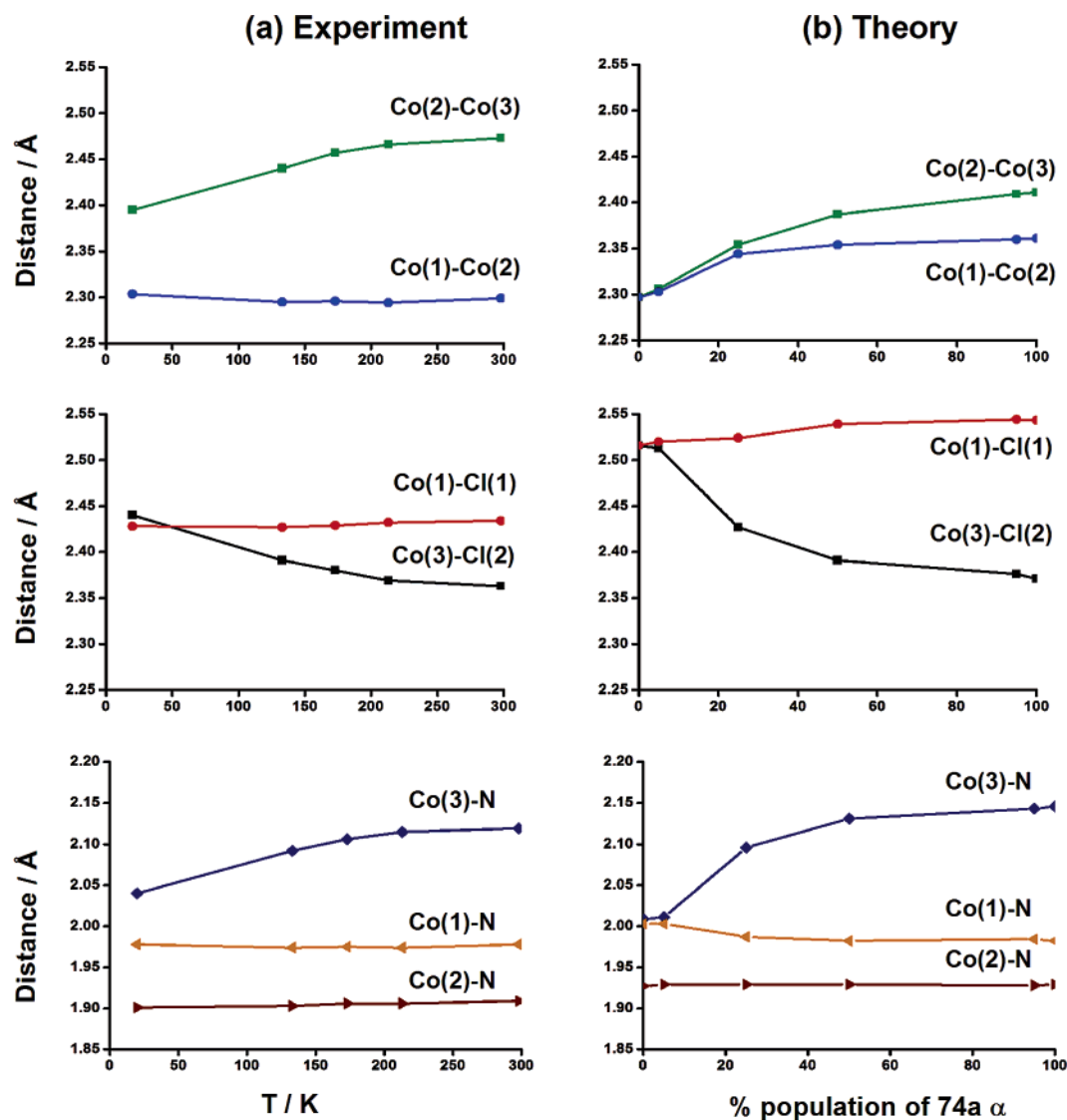


Figure 6. Variation of the Co–Co, Co–Cl, and Co–N bond lengths of $\text{Co}_3(\text{dpa})_4\text{Cl}_2$ with (a) temperature (experiment) and (b) occupancy of the 74a α orbital in the ^2B state (theory).

of the symmetric ^2B minimum) to 0.0:1.0. The changes in the key structural parameters as the population of the 74a α orbital is increased are summarized in Figure 6, where the temperature dependence of the crystallographically determined parameters is reproduced for comparison. The similarity between computed and crystallographic data is quite remarkable, even down to the elongation of the Co(3)–Cl(2) bond observed at low temperatures. On this basis, we are confident that the observed changes in the bond lengths of $u\text{-Co}_3(\text{dpa})_4\text{Cl}_2$ as the temperature is reduced are indicative of variable distribution of Co(3) $d_{x^2-y^2}$ character between the occupied and vacant manifolds, a situation that can arise *only* in the ^2B state.

Summary: Overview of the Structural Chemistry of $\text{Co}_3(\text{dpa})_4\text{Cl}_2$. In summary, *three* distinct electronic states, ^2A , ^4B , and ^2B , are required to rationalize the complex structural chemistry of the $\text{Co}_3(\text{dpa})_4\text{Cl}_2$ system. The energetic separation between these states is small, so environmental effects, such as temperature or solvent of crystallization, can significantly perturb the shape of the potential energy surface. The structural and magnetic properties of $s\text{-Co}_3(\text{dpa})_4\text{Cl}_2$ and the high-temperature form of $u\text{-Co}_3(\text{dpa})_4\text{Cl}_2$ can readily be explained in terms of

two spin-state isomers, ^2A and ^4B . However, the minima for these two states are well-defined and lie in very different regions of multidimensional space, and so a model based on these two alone cannot account for the temperature dependence of the structural parameters. We propose that below 200 K, a spin-crossover from the ^4B potential energy surface to a second doublet state, ^2B , occurs, effectively “short-circuiting” the region of multidimensional space where both ^2A and ^4B states are very unstable. The electronic structure of the ^2B state is unique in allowing a continuous variation in Co(3)–N bond lengths because the vacancy in the 74a α orbital allows Co(3) $d_{x^2-y^2}$ character to be distributed between occupied and vacant manifolds. The very flat ^2B potential energy surface allows changes in lattice strain (brought about by varying the temperature) to induce significant changes in molecular structure.

Finally, we return to the question posed in the Introduction: does the structural chemistry of the $\text{Co}_3(\text{dpa})_4\text{Cl}_2$ constitute a genuine example of bond-stretch isomerism? The high-temperature forms of $s\text{-}$ and $u\text{-Co}_3(\text{dpa})_4\text{Cl}_2$ differ in their ground-state multiplicity (doublet and quartet, respectively), and so are more accurately described as spin-state, rather than bond-stretch,

isomers. The situation within the doublet manifold is rather less clear-cut. As we noted above, the 2A and 2^2A states fulfill all the criteria laid down for bond-stretch isomers in the original work of Hoffman;^{9a} the two states share the same ground-state multiplicity and are related by a formal two-electron excitation. However, as the 2^2A state plays no role in our model for the structural chemistry, its identification as a bond-stretch isomer of the symmetric 2A ground state is somewhat academic. The relationship between the 2A and 2B states also fulfills the multiplicity criterion for bond-stretch isomers, but the *minima* on the two surfaces are in fact very similar (both are symmetric). Indeed, none of the structures that we assign to the 2B potential energy surface (u-Co₃(dpa)₄Cl₂ below 200 K) actually corresponds to the minimum, but rather to a very flat region between the symmetric and unsymmetric limits. In this system, then, the term bond-stretch isomerism is an oversimplification that obscures the complex redistribution of electron density that causes the polymorphism.

Computational Methods

All calculations described in this paper were performed using the Amsterdam Density Functional package (ADF2004.01).²⁰ A double- ζ Slater-type basis set, extended with a single polarization function, was used to describe the main group atoms, while cobalt was modeled with a triple- ζ basis set. Electrons in orbitals up to and including 1s

(20) ADF2004.01; Baerends, E. J.; et al. SCM: Amsterdam, 2004.

{C, N}, 2p{Cl}, and 3p {Co} were considered part of the core and treated in accordance with the frozen core approximation. The local density approximation was employed for the optimizations,²¹ along with the local exchange–correlation potential of Vosko, Wilk, and Nusair²² and gradient corrections to exchange and correlation proposed by Becke and Perdew (BP86).¹³ The ADF program does not support the C_4 point group, so all calculations were in fact performed using C_2 symmetry. For orbitally degenerate states (2E , 4E), convergence to a C_4 -symmetric structure was achieved by distributing a single electron equally between the two components of the degenerate e orbital (both transform as b in the C_2 point group). Different configurations were defined using the “occupations” key. The converged geometry and electron density at the BP86 level were used to compute energies with the B3LYP and VS98 functionals. All structures were optimized using the gradient algorithm of Versluis and Ziegler.²³

Acknowledgment. We thank the EPSRC (GR/R74963/01) for financial support.

Supporting Information Available: Optimized Cartesian coordinates and total energies of the 2A , 4A , 4B , 2^2A , and 2B states. Complete ref 20. This material is available free of charge via the Internet at <http://pubs.acs.org>.

JA0581402

(21) Parr, R. G.; Yang, W. *Density Functional Theory of Atoms and Molecules*; Oxford University Press: New York, 1989.

(22) Vosko, S. H.; Wilk, L.; Nusair, M. *Can. J. Phys.* **1980**, *58*, 1200.

(23) Versluis, L.; Ziegler, T. *J. Chem. Phys.* **1988**, *88*, 322.